

# Modeling of ions energy distribution profile of electronegative plasma discharges with an efficient Monte Carlo simulator

M. Ardehali

Silicon Systems Research Laboratories, NEC Corporation,  
Sagamihara, Kanagawa 229 Japan

## Abstract

The crucial role that Ions Energy Distribution Function (IEDF) at the electrodes plays in plasma processing of semiconductor materials demands that this quantity be predicted with high accuracy and with low noise levels in any plasma simulator. In this work, an efficient Particle-in-cell/Monte-Carlo (PIC/MC) simulator is developed to model IEDF at the electrodes of electronegative plasma discharges. The simulator uses an effective method to increase the number of MC particles in regions of low particle density by splitting the particles and by adjusting their statistical weight. This statistical enhancement technique, which does not require interprocessor communication, is particularly suitable for parallel processing. The simulator is used to model an electronegative rf discharge at a pressure of 25 mTorr. The IEDF obtained from this simulator has good statistics with low noise levels, whereas the IEDF calculated by standard PIC/MC simulator is jammed with stochastic noise.

## I. Introduction

Radio frequency glow discharges are widely used in microelectronics for deposition and etching thin solid films and for Ultra Large Scale Integrated (ULSI) circuit fabrication [1]. The understanding of these discharges is of considerable importance for a better control and optimization of semiconductor processing. Unfortunately, these discharges are complex systems that are very difficult to analyze [2-4]. In the last few years, Particle-In-Cell/Monte-Carlo (PIC/MC) simulation has been used successfully to model rf discharges. PIC/MC technique combines the microscopic transport of electrons and ions with the self consistent electric field. The technique is very attractive because it can handle the nonlocal effects which are dominant at low pressures without making any *ad hoc* assumptions [5-6]. Furthermore, the PIC/MC technique is capable of predicting ions energy distribution function at electrode surfaces.

Unfortunately, PIC/MC simulation of RIE discharges suffers from significant noise which is inherently associated with regions of low particle density. In particular, because the particle density in the sheath is many orders of magnitude smaller than in the bulk, the MC noise inevitably associated with the sheath is considerably larger than the noise associated with the bulk. Several techniques have been proposed to improve the sampling within the sheath [7-9]. However, even with the improved sampling techniques, the present PIC/MC simulators suffer from intensive computational requirements and from excessive noise associated with the sheath. Serious problems arise from the noise within the sheath and they may threaten the reliability of the simulation data.

## II. Details of simulation

Since the motion of electrons and ions in rf discharges under the influence of self-consistent electric field bears some resemblance to the motion of electrons and holes in semiconductor devices, the advanced techniques that have been developed for device simulation [10-12] may also be useful for plasma simulation. For example, for hot electron injection in MOSFETs [13], only one out of  $10^{10}$  channel electrons makes a contribution to the gate current. A straight forward MC simulation is extremely expensive, requiring the simulation of billions of cold MC particles. To reduce the simulation cost of these problems, Phillips and Price [10] divided the domain of the electron states  $S$  into a rare part  $R$  and a complementary common part  $C$ . When a particle enters  $R$  from  $C$ , its state is stored. The rare portion of the particle history is then repeated for a fixed number of  $N$  times starting from the same initial condition. After  $N$  repetitions, the MC simulation continues in the  $C$  domain using only one of the  $N$  rare trajectories. Obviously, in calculating the average values, a weight of  $1/N$  is given to the results in  $R$ .

Motivated by their work, we use a similar technique to increase the number of MC particles in the sheath by splitting the particles in regions of low particle

density. There are, however, some fundamental differences between this work and that of [10-12]. In particular, in the work of Phillips and Price, the energy components of the particles are weighed differently, whereas in the present work, as is shown in part III, the spatial components of the particles are weighed differently.

There are also some important differences between this work and the previous plasma simulation works that increase the number of MC particles within the sheath [14-16]. For example, in the work of Goto *et. al.* [16], the discharge is divided into many slabs and every slab consists of  $M_s$  sub-slabs. Each sub-slab in turn is divided into  $M_f$  fine-sub-slabs in which the generation and loss of particles are counted. The number of particles in every fine-sub-slab is set to a *standard* number  $N_s$ . When the simulated particle number of a slab exceeds  $1.4M_sM_fN_s$ , the number of particles of all fine-sub-slabs in the slab is counted. If the particle number of a fine-sub-slab is greater than  $N_s$ , then it is reduced to  $N_s$ . Thus in their work, as well as in Refs. [14-15], an attempt is made to set the number of particles in every fine-sub-slab or in every cell equal to a constant number  $N_s$ . In contrast, in this work, the discharge is not divided into slabs, sub-slabs, and fine-sub-slabs, and no attempt is made to set the number of particles in every cell or in every fine-sub-slab equal to a standard number. In the present work, a suitable weight  $W_i$  is associated with each cell  $i$  which is automatically updated with every time step, and unlike Refs. [14-16], the particles are split when the particle's weight is significantly larger than the weight associated with the cell. In this respect the present work is similar to the splitting technique used in the device simulation [10-12].

### III. Simulation of electronegative discharge with SPLIT-PIC/MC technique

A question of fundamental interest is whether the SPLIT technique, which was applied to electropositive discharges [17], can also be used to improve the statistics of electronegative simulators. To address this question, we developed a simulator to model electronegative gases [18-20] using SPLIT technique. The present simulator uses an effective method to increase of the number of MC particles in regions of low particle density by splitting the particles and by adjusting their statistical weight. The computation time for splitting the MC particles is very small and in general is less than 5% of the total calculation time. Using this splitting technique, the number of MC particles within the sheath becomes of the same order as in the bulk. In contrast, in the standard PIC/MC simulation, even though the sheath is the most important region in the discharge and has a profound influence on the properties of the bounded plasma, the number of MC particles in the sheath is many orders of magnitude smaller than in the bulk.

Very briefly, the present SPLIT- PIC/MC simulator consists of the following steps:

- (1) Each cell  $i$  contains a suitable weight  $W_i$  which is automatically updated with time.
- (2) The instantaneous locations of MC particles representing ions and electrons are interpolated to the grid points to obtain the charge density.
- (3) Poisson's equation on a spatially discretized mesh is solved to obtain the electric field.
- (4) The electric field is interpolated from the grid points to the location of MC particles.
- (5) The equations of motion under the local and instantaneous electric field are integrated.
- (6) When ion  $j$  enters cell  $i$ , its weight  $m_j$  is compared with  $W_i$ . If the particle's weight is much heavier than  $W_i$ , then it splits into two sub-particles, each with weight  $\frac{m_j}{2}$ .
- (7) Random numbers (Monte Carlos technique) and collision cross sections are used to determine the probability that each particle suffers a collision.

It is worth noting that the present SPLIT-PIC/MC simulator is particularly suitable for parallelization and vectorization. The SPLIT method does not use the distribution of particle weights in a cell to adjust the number of MC particles to a desired population. Since the SPLIT technique does not require fetching particle data handled by other processors, there is no need for inter-processor communication, and complete parallelization with respect to particles is achieved. The numerical results presented here were all performed on an NEC parallel machine Cenju-3 (16 processor) which has a VR4400SC (75 MHz) processor and 64MB local memory in each processor [21].

To examine the effectiveness of SPLIT technique, we have modeled an electronegative rf plasma at a pressure of 25 mTorr both with the SPLIT-PIC/MC simulator and with the standard PIC/MC simulator [22]. The simulator is based on a Chlorine-like gas. The processes considered are ionization leading to positive ion formation, dissociative electron attachment leading to negative ion formation, and positive ion/negative ion recombination leading to positive and negative ions removal. These processes are represented as follows:



where  $Cl_2^+$  and  $Cl^-$  are the main positive and negative ions respectively. In the simulation, the left electrode is driven with a voltage  $V_{rf}(t) = V_{rf} \sin \omega t$ , where  $V_{rf} = 300$  Volts, the applied frequency is  $\frac{\omega}{2\pi} = 10$  MHz, and the discharge length is 10 cm with perfectly absorbing electrodes. The time step  $\delta t = 0.1$  ns which is small enough to resolve the electron plasma frequency.

Since in this work we are primarily interested in testing the effectiveness and usefulness of SPLIT-PIC/MC simulator, we have intentionally kept the model of the plasma simple. The electron-neutral processes consist of elastic

scattering and ionization. The total electron-neutral scattering cross section  $\sigma_{total}(v)$  is given by  $\sigma_{total}(v) = \frac{K_{total}}{v}$ , where  $v$  is the electron velocity and the rate constant  $K_{total}$  is  $5 \times 10^{-8} \text{ cm}^3/\text{s}$  [5]. Ionizing collisions occur if the electron energy is larger than 16 eV. An ionizing collision [Eq. (1)] is modeled by loading a new electron and ion at the position of the ionizing electron. The kinetic energy after ionizing collision is partitioned between the two electrons with equal probability. The cross section for ion-neutral charge-exchange collision is  $\sigma_{ce}(v) = 1 \times 10^{-15} \text{ cm}^2$  [5]. After charge exchange collision, the ion is scattered isotropically, with its energy being set at the background temperature. Since the rate constant for attachment  $K_{at}$  is constant [18], the cross section for attachment [Eq. (2)] is modeled as  $\sigma_{at}(v) = \frac{K_{at}}{v}$  where  $K_{at} = 1.8 \times 10^{-10} \text{ cm}^3/\text{s}$  [18]. The attachment reaction is modeled by removing the electron from the system and by loading a negative ion at the position of the attaching electron. The kinetic energy of the generated negative ion is set at the background temperature. Finally because the rate constant for recombination  $K_{at}$  is also constant, the cross section for recombination [Eq. (3)] is modeled as  $\sigma_{rec}(v) = \frac{K_{rec}}{v_{ion}}$ , where  $K_{rec} = 5 \times 10^{-8} \text{ cm}^3/\text{s}$  [18], and  $v_{ion}$  is the velocity of the recombining ion. The recombination reaction is modeled by removing positive and negative ions from the system. Simulation results have shown that the splitting technique leads to reduction of noise within the sheath no matter what the detailed forms of the cross sections are.

## IV. Results and discussion

The simulation is started by loading a few hundred *quiet* particles uniformly between the electrodes. Initially the velocity of all particles, negative ions, positive ions and electrons, is set to zero and the density of positive ions is set equal to the density of negative ions and electrons. Since the mass of electrons is much smaller than the mass of ions, electrons rapidly leave the system and sheaths develop at the boundaries. The density of electrons and ions continues to rise by ionization until steady state is reached where the ionization rate becomes equal to the total loss rate. At steady state the number of electrons and ions approaches a constant value. With SPLIT-PIC/MC technique, the simulator approaches steady state after approximately 900 cycles, whereas with the standard PIC/MC simulator, more than 2000 cycles are required for the simulator to arrive at steady state.

To clearly demonstrate the effectiveness of the SPLIT technique, we ran SPLIT-PIC/MC simulator for approximately 1000 cycles, while we ran the standard PIC/MC simulator for approximately 3000 cycles. Since the process of splitting particles takes less than 5% of the calculation time, the total computation time for the SPLIT simulator is approximately three times smaller than for the standard simulator. As shown below, even with 66% smaller computation time, the simulation results obtained from SPLIT-PIC/MC simulator are more

accurate and have lower noise levels than the results obtained from the standard PIC/MC simulator.

Figures 1 (a) and 1 (b) show the number of MC particles for positive ions obtained from the SPLIT-PIC/MC simulator and from the standard PIC/MC simulator (in relative units). The important point to notice is that for SPLIT-PIC/MC simulator, the number of MC particles in the sheath is of the same order of magnitude as in the bulk. In contrast, for the standard PIC/MC simulator, the number of MC particles in the sheath is many orders of magnitudes smaller than in the bulk.

Figures 2 (a) and 2 (b) show the instantaneous (not averaged over several period) positive ion density in log scale obtained from the SPLIT-PIC/MC simulator and from the standard PIC/MC simulator. Note that the massive ions do not respond to the rapid variations of the electric field and hence the ion density profile is nearly time independent. Figs. 2 (a) and 2 (b) clearly indicate that SPLIT technique leads to significant reduction of MC noise within the sheath. Figure 2 (c) shows the positive ion density profile within the sheath in linear scale simulated by the standard PIC/MC technique (dashed) and by the SPLIT-PIC/MC technique (line). Comparing the two cases, it can be seen that the PIC/MC profile is zero within several cells, whereas the SPLIT-PIC/MC profile is never zero within any cells and has a much smaller noise level.

Figure 3 shows the instantaneous profile of negative ion density within the discharge simulated by SPLIT-PIC/MC technique. The negative ions are confined to the bulk of the discharge and are completely excluded from the sheath by the large sheath electric field.

Figures 4 (a) and 4 (b) show the instantaneous positive ion phase-space simulated by the SPLIT-PIC/MC technique and by the standard PIC/MC technique. These figures clearly show that the ions are accelerated by the sheath electric field. The ions that suffer several collisions arrive at the electrode with very small energies. In contrast, the ions that do not suffer any collisions arrive at the electrode by the average sheath potential. The important point about these figures is that the SPLIT-PIC/MC simulator dramatically increases the number of ions within the sheath, hence leading to significant reduction of MC noise in regions of low particle density.

As another example of the effectiveness of SPLIT technique, the variation of the electric field within the discharge at phase  $\frac{3\pi}{2}$  is simulated both by the SPLIT-PIC/MC [Fig. 5 (a)] technique and by the standard PIC/MC [Fig. 5 (b)] technique. Due to disparity between electrons and ions masses, electrons rapidly leave the system and large electric fields develop near the electrodes. The electric field in the bulk of the discharge, however, is much smaller than in the sheath, indicating that the net charge density within the bulk is very small. The large electric field at the electrode boundaries effectively pushes the negative ions out of the sheath (see Fig. 3). Figure 5 (a) clearly demonstrates that SPLIT-PIC/MC technique, by increasing the number of MC particles within

the sheath, dramatically reduces the noise associated with the sheath electric field [it should be emphasized that these figures *are not* averaged over many periods, rather they represent the snapshot or the instantaneous electric field. Furthermore, the computation time for Fig. 5 (b) is three times larger than for Fig. 5 (a)].

To demonstrate that the present SPLIT-PIC/MC simulator can predict the physical properties of the electronegative discharges, in Figs. 6 (a) and 6 (b), we present positive and negative ion current densities averaged over 50 periods and at four times during the rf cycle. (In contrast to Figs. 2-5, Figs. 6(a) and 6 (b) are averaged over many periods and are not instantaneous). Note that the negative ion current density is almost one order of magnitude smaller than the positive ion current density. Furthermore, since negative ions are excluded from the sheath, the negative ion flux within the sheath is almost zero. In contrast, positive ions are accelerated by the sheath electric field and positive ion flux increases sharply within the sheath.

Figures 2-5 have clearly shown the effectiveness of SPLIT-PIC/MC simulator for improving the statistics of ion density and the discharge electric field. However, from the point of view of semiconductor processing, the most important characteristic of RIE discharges is the Ions Energy Distribution Function (IEDF) at the surface of the electrodes [23, 24]. Thus a question of fundamental interest is whether the SPLIT technique can improve the statistics of IEDF at the electrodes (the question of the effectiveness of SPLIT technique on IEDFs at the electrodes was not considered in [17]). To answer this question, we simulated the IEDF both by the standard technique and by the SPLIT technique. The IEDF obtained from the SPLIT-PIC/MC simulator and from the standard PIC/MC simulator are shown in Figs 7 (a) and 7 (b). Figure 7 (a) is obtained after running SPLIT-PIC/MC simulator for 950 periods, whereas Fig. 7 (b) is calculated after running PIC/MC simulator for 3000 periods; however, in both Figs. 7 (a) and 7 (b), the IEDFs are time averaged over 50 periods. The IEDF at the electrode consists of a few spikes that are superimposed on a collisional background. Although most ions have many collisions in the sheath and hence create the collisional background profile, a few ions have only several charge-exchange collisions, creating the spikes in the profile. Comparing Figs. 7 (a) and 7 (b), it can be seen that with the standard PIC/MC simulator, the statistics of IEDF is very poor, jammed with stochastic noise; whereas with the SPLIT-PIC/MC simulator, the statistics of IEDF is significantly enhanced and has a much lower noise level. To further demonstrate the effectiveness of the SPLIT technique, in Figs. 7 (c) and 7 (d), we present the IEDF at the electrode simulated by the standard PIC/MC technique and time averaged over 150 and 600 periods respectively. Note that Fig. 7 (a) which is obtained from SPLIT-PIC/MC simulator and is time averaged over only 50 period is smoother than Fig. 7 (d) which is obtained from the standard PIC/MC simulator and is time averaged over 600 periods. These figures clearly demonstrate that SPLIT technique leads to dramatic reduction of stochastic noise in IEDF at the electrodes.

## V. Conclusion

A stable algorithm which is highly suitable for parallelization and vectorization is developed to simulate electronegative rf discharges. The algorithm splits Monte-Carlo particles in regions of low particle density and hence improves the sampling and reduces the noise inherently associated with the sheath. The process of splitting the particles takes only a very small fraction (less than 5%) of the total computation time. The most attractive feature of SPLIT technique is that it can dramatically reduce the noise associated with the IEDF at the electrode. In particular, the IEDF at the electrode obtained from SPLIT-PIC/MC simulator and averaged over 50 periods has a better statistics and lower noise level than the distribution function obtained from the standard PIC/MC simulator and averaged over 600 periods. The SPLIT-PIC/MC simulator shows great promise for modeling any kind of bounded plasmas where sheaths inevitably develop, and for calculating IEDF at the electrodes of more complex discharges (such as ECR or ICP) in two or three dimensions.

## References

- [1] M. A. Lieberman and R. A. Gottscho, "Design of high density plasma sources for material processing," in *Physics of Thin Films*, M. Francombe and J. Vossen, Eds. New York: Academic, 1993.
- [2] E. Gogolides, J. P. Nicolai, and H. H. Sawin, "Comparison of experimental measurements and model predictions for radio-frequency Ar and  $SF_6$  discharges," *J. Vac. Sci. Technol. A*, vol. A7, no. 3, pp. 1001-1005, 1989.
- [3] E. Gogolides, and H. H. Sawin, "Continuum modeling of radio-frequency glow discharges. I. Theory and results for electropositive and electronegative gases," *J. Appl. Phys.*, vol 72, pp. 3971-3987, 1992.
- [4] E. Gogolides, and H. H. Sawin, "Continuum modeling of radio-frequency glow discharges. II. Parametric studies and sensitivity analysis," *J. Appl. Phys.*, vol 72, pp. 3988,4002, 1992.
- [5] D. Vender and R. W. Boswell, "Numerical modeling of low-pressure rf plasmas," *IEEE Trans. Plasma Sci.*, vol. 18, pp 725-732, 1990.
- [6] M. Surendra and D. B. Graves, "Particle simulation of rf glow discharges," *IEEE Trans. Plasma Sci.*, vol. 19, pp. 144-157, 1990.
- [7] A. Date, K. Kitamori, S. Sakai, and H. Tagashira, "Self- consistent Monte Carlo modeling of RF plasma in a helium-like model gas," *J. Phys. D.*, vol. 25, pp 442-453, 1992.
- [8] P. L. G. Ventzek and K. Kitamori, "Higher-order sampling strategies in Monte Carlo simulations of electron energy distribution functions in plasmas," *J. Appl. Phys.*, vol. 75, pp. 3785-3788, 1994.
- [9] K. Nanbu, "Fourier transform method to determine the probability density function from a given set of random samples," *Phys. Rev. E*, vol. 52, pp. 5832-5838, 1995.
- [10] A. Phillips and P. J. Price, "Monte Carlo calculations of hot electron energy tails," *Appl. Phys. Lett.*, vol. 30, pp. 528-530, 1977.
- [11] F. Venturi, R. K. Smith, E. C. Sangiorgi, M. R. Pinto, and B. Ricco, "A general purpose device simulator coupling Poisson and Monte Carlo transport with applications to Deep submicron MOSFET's," *IEEE Trans. Com-Aided Design*, vol. 8, pp. 360-369, 1989.
- [12] E. Sangiorgi, B. Ricco, and F. Venturi, "MOS<sup>2</sup>: An efficient Monte Carlo simulator for MOS devices," *IEEE Trans. Com-Aided Design*, vol. 7, pp. 259-271, 1988.

- [13] T. H. Ning, P. W. Cook, R. H. Dennard, C. M. Osburn, S. E. Shuster, and N. H. Yu, "  $1\mu\text{m}$  MOSFET VLSI technology: Part. IV- hot-electron design constraints," *IEEE Trans. Electron Devices*, vol. ED-32, pp. 783-787, 1985.
- [14] H. W. Trombley, F. L. Terry, and M. E. Elta, "A self-consistent particle model for the simulation of RF glow discharges," *IEEE Trans. Plasma Sci.*, vol. 19, pp. 158-162, 1991.
- [15] R. Krimke and H. M. Urbassek, "Influence of plasma extraction on a cylindrical low-pressure RF discharge: A PIC-MC study," *IEEE Trans. Plasma Sci.*, vol. 23, pp. 103-109, 1995.
- [16] M. Goto, Y. Kondoh, and A. Matsuoka, "Monte-Carlo simulation of discharge plasmas using fine-sub-slabs," *Proc. of the 3rd Int. Conf. on reactive plasmas*, Nara, Japan, pp. 116-117, 1997.
- [17] M. Ardehali and H. Matsumoto, "An efficient Monte Carlos simulator for electropositive discharges," *IEEE Trans. Plasma-Sci.*, vol. 25, no. 5, pp. 1081-1085, 1997.
- [18] S. Park and D. J. Economou, "Analysis of low pressure RF glow discharges using a continuum model," *J. Appl. Phys.*, vol. 68, pp. 3904-3915, 1990; S. Park and D. J. Economou, "Parametric study of a radio-frequency glow discharge using a continuum model," *Ibid*, vol. 68, pp. 4888-4890, 1990.
- [19] M. Meyyappan, "Analysis of magnetron electronegative rf discharge," *J. Appl. Phys.*, vol. 71, pp. 2574-2579, 1992.
- [20] D. P. Lymberopoulos and D. J. Economou, "Modeling and simulation of glow discharge plasma reactors," *J. Vac. Sci. Technol. A*, vol. 12, pp. 1229-1236, 1994.
- [21] K. Muramatsu, S. Doi, T. Washio, and T. Nakata, "Cenju-3 parallel computer and its application to CFD," in *Proceedings of the 1994 international symposium on parallel architectures, algorithms and networks (ISPAN)*, pp. 318-325, 1994.
- [22] M. Ardehali, "Analysis of low pressure electro-positive and electro-negative rf plasmas with Monte Carlo method". Manuscript can be obtained from physics@xxx.lanl.gov; Paper: physics/9810027.
- [23] R. A. Gottscho, "Ion transport anisotropy in low pressure, high density plasmas," *J. Vac. Sci. Technol. B*, vol. 11, pp. 1884-1889, 1993.
- [24] R. A. Gottscho, C. J. Jurgensen, and D. J. Vitkavage, "Microscopic uniformity in plasma etching," *J. Vac. Sci. Technol. B*, vol. 10, pp. 2133-2147, 1992.

## Figure Captions

**Important Note:** All figures should be considered from left to right and top to bottom.

Figures 1 (a), 1 (b), are on the same page.

Figures 2 (a), 2 (b), and 2 (c) are on the same page.

Figure 3 is on one page.

Figures 4 (a) and 4 (b) are on the same page.

Figures 5 (a) and 5 (b) are on the same page.

Figures 6 (a) and 6 (b) are on the same page.

Figures 7 (a) and 7 (b) are on the same page.

Figures 7 (c) and 7 (d) are on the same page.

**Fig. 1 (a)** - Number of MC particles for ions obtained from SPLIT-PIC/MC simulator. Simulation conditions:  $V_{rf} = 300$  Volts,  $\frac{\omega}{2\pi} = 10$ , pressure 25 mTorr.

These conditions apply to all figures. In Figs. [1-6],  $x = 0$  (left electrode) is the powered electrode and  $x = 10$  (right electrode) is the grounded electrode.

**Fig. 1 (b)** - Number of MC particles for ions obtained from the standard PIC/MC simulator.

**Fig. 2 (a)** - Instantaneous ion density obtained from SPLIT-PIC/MC simulator in log scale.

**Fig. 2 (b)** - Instantaneous ion density obtained from the standard PIC/MC simulator in log scale.

**Fig. 2 (c)** - Instantaneous ion density in the sheath from PIC/MC simulator (dashed) and from SPLIT-PIC/MC simulator (line).

**Fig. 3** - Instantaneous negative ion density within the discharge obtained from SPLIT-PIC/MC technique in log scale.

**Fig. 4 (a)** - Ion phase space diagram obtained from SPLIT-PIC/MC simulator.

**Fig. 4 (b)** - Ion phase space diagram obtained from the standard PIC/MC simulator.

**Fig. 5 (a)** - Instantaneous electric field at phase  $\frac{3\pi}{2}$  obtained from SPLIT-PIC/MC simulator.

**Fig. 5 (b)** - Instantaneous electric field at phase  $\frac{3\pi}{2}$  obtained from PIC/MC simulator.

**Fig. 6 (a)** - Positive ion current density averaged over 50 periods at 4 times during the rf cycle. For Figs. 6 (a) and 6 (b)  $\frac{\omega t}{2\pi} = 0$  (solid line),  $\frac{\omega t}{2\pi} = 0.25$  (dotted line),  $\frac{\omega t}{2\pi} = 0.5$  (dashed-dashed line),  $\frac{\omega t}{2\pi} = 0.75$  (dashed line).

**Fig. 6 (b)** - Same as Fig. 6 (a) but for negative ion current density.

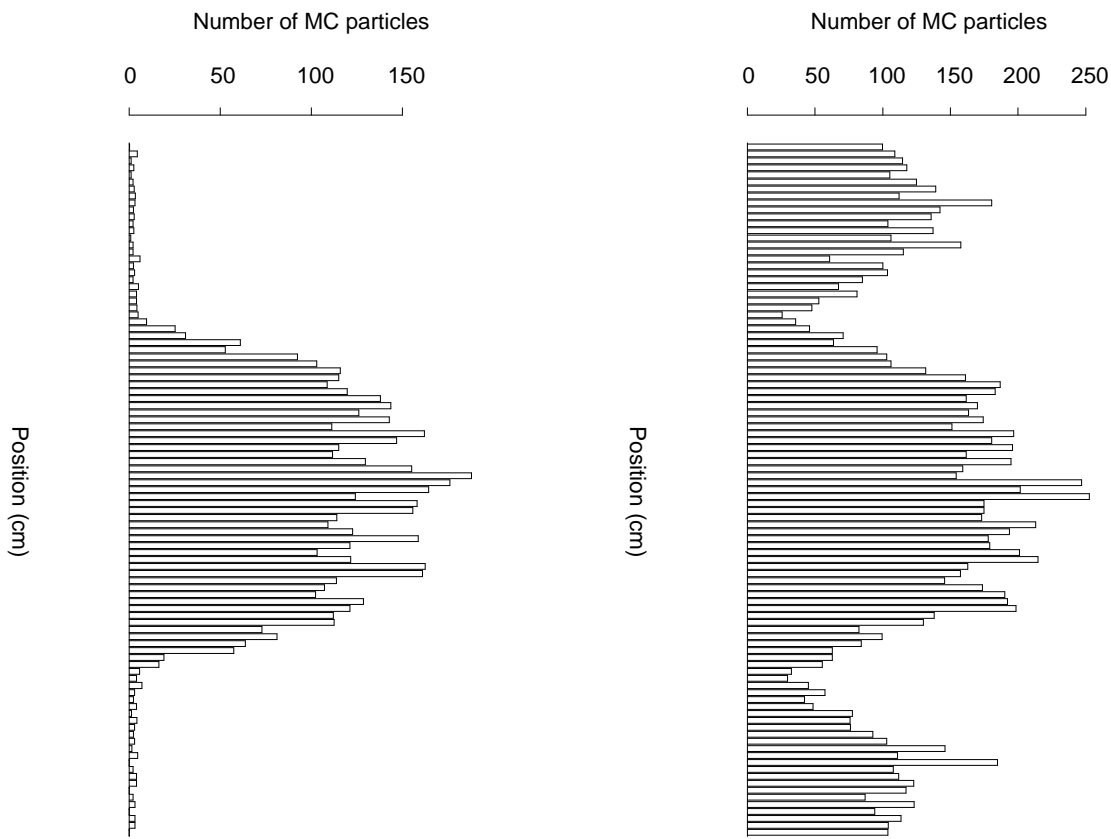
**Fig. 7 (a)** - Ions energy distribution profile at the electrode obtained from SPLIT-PIC/MC simulator after running the simulator for 1000 periods and averaging over 50 periods. In Figs. [7 (a), 7 (b), 7 (c), and 7 (d)], the horizontal axis represents the energy of ion striking the electrode, and the vertical axis represents the distribution of ions energy.

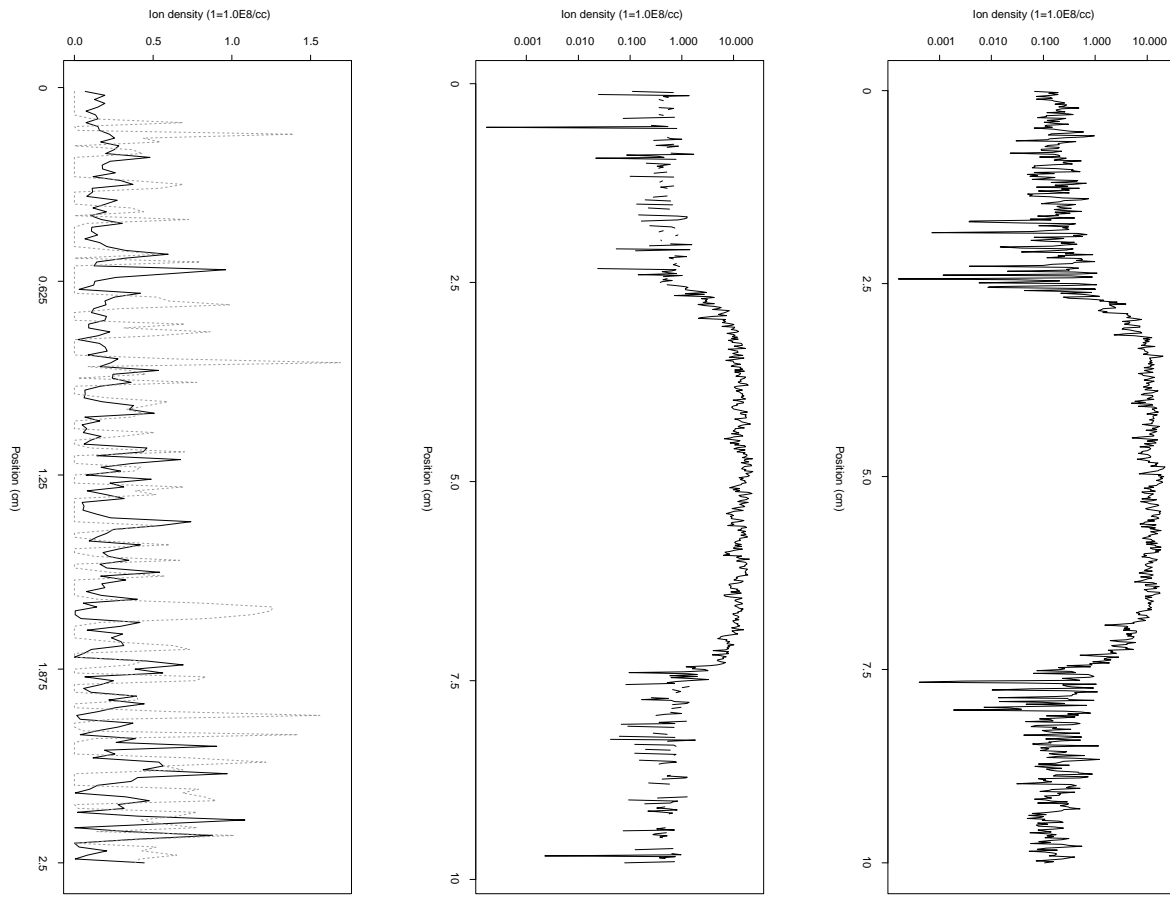
**Fig. 7 (b)** - Ions energy distribution profile at the electrode obtained from PIC/MC simulator after running the simulator for 3000 periods and averaging

over 50 periods.

**Fig. 7 (c)** - Ions energy distribuion profile at the electrode obtained from PIC/MC simulator after running the simulator for 3000 periods and averaging over 150 periods.

**Fig. 7 (d)** - Ions energy distribuion profile at the electrode obtained from PIC/MC simulator after running the simulator for 3000 periods and averaging over 600 periods.





Negative ion density ( $1=1.0E8/cc$ )

